10th Annual AIAA Aviation Technology, Integration, and Operations Conference, 13-15 September 2010,
Fort Worth, Texas.

A Novel Configuration for Future Narrowbody Aircraft Utilizing Natural Laminar Flow and Open Fan Technologies

Phillip C. Adkins*, Todd W. Erickson†, Darin J. Gaytan‡, Sina S. Golshany§, Keith K. Holmlund‡, Kristina L. Larson‡, Devin J. Lewis**, Chris N. Nsavu‡, John D. Roehrick††, and Michael J. Zarem‡
University of Southern California, Los Angeles, CA, 90007

The next generation of medium range commercial transport aircraft is considered to be the focal point of present-day research in the commercial aviation industry. The expected increase in oil price, the possible introduction of a carbon tax, and stricter environmental constraints have made the development of more efficient and environmentally compatible commercial aircraft necessary to replace the aging fleet of Boeing 737s and Airbus A320s. Egret attempts to address these issues by integrating modern concepts, such as natural laminar flow, bleedless open fan engines that use alternative fuels, composite load bearing structure, and ultra-high aspect ratio folding wings that provide compatibility with current airport infrastructure while increasing overall aerodynamic efficiency. The resulting design presents tremendous improvements over today's operating commercial aircraft technology. As a result, Egret attains a 25% increase in cruise L/D, 25% reduction of SFC, and a 38% reduction in direct operating cost.

Nomenclature

A	=	Blade wetted area in m^2
AR	=	Aspect ratio
C_D	=	Drag coefficient
C_{Dblade}	=	Average blade drag coefficient
C_{ENVTAX}	=	Cost associated with environmental taxation
C_L	=	Lift coefficient
C_{Lmax}	=	Maximum lift coefficient
D_p	=	Propeller diameter in m
L/D	=	Lift-to-drag ratio
Λ_{LE}	=	Leading edge wing sweep angle in degrees
M_b	=	Blade mass in kg
M_{DD}	=	Drag divergence Mach number
M_i	=	Normalized emission multiplier in fraction of effect of CO_2
Ω	=	Phillip's angle; impingement angle of a released blade
P_1,P_2	=	Aftward (1) and radial (2) quadratic drag force coefficient in kg/m
P_3	=	Combustor inlet pressure in kPa
Re_{tr}	=	Reynolds number corresponding to the chordwise transition to turbulence
ϱ	=	Density
S_{NOx}	=	NOx severity index
T_3	=	Combustor inlet temperature in Kelvins
$v_{0,plane}$	=	Forward velocity of the aircraft in m/s
$v_{0,prop}$	=	Initial tangential blade velocity at blade center of mass in m/s
war	=	Water-to-air ratio
W_{fix}	=	Fixed equipment weight in lbs
$W_{F,max}$	=	Maximum fuel weight in lbs
W_{PP}	=	Power plant weight in lbs
$W_{Structure}$	=	Structure weight in lbs

* Physics and Astronomy, AIAA Member
† Mechanical Engineering, Boeing Commercial Airplanes, AIAA Member
‡ Aerospace Engineering, AIAA Member
§ Aerospace Engineering, Boeing Commercial Airplanes, AIAA Member
** Architecture, AIAA Member
†† Mechanical Engineering, AIAA Member

I. Introduction

RESPONDING to AIAA's Request for Proposal (RFP), The University of Southern California's Advanced Commercial Concepts Group (UACC) developed and submitted proposals for a family of concepts for a fuel efficient and environmentally friendly medium haul commercial aircraft. Intended for a service entry date of 2020, the new designs would serve as Boeing 737 and Airbus A320 replacements, closely replicating the present day challenges faced by the aerospace industry. These challenges include the expected increase in oil price, the possible introduction of a carbon tax, and the tightening of other environmental constraints. UACC's Egret attempts to address these issues by integrating novel concepts, such as natural laminar flow (NLF), bleedless open fan engines that use alternative fuels, composite load bearing structure, and ultra-high aspect ratio folding wings that provide compatibility with current airport infrastructure while increasing overall aerodynamic efficiency.

II. Design Methodology

The general design philosophy of Egret has been substantially influenced by methodology presented by Jan Roskam [1] and Edward Heinemann [2]. Special emphasis was placed on configuring a safe and failure tolerant platform. Simultaneously, the design effort was concentrated on satisfying relevant in-place federal regulations and industry standards regarding emissions, noise, and survivability. New technologies were only integrated if they could be supported by the establishment of a valid business case with minimum development risk and maximum market compatibility.

Facing challenging design problems, techniques outlined by the general literature and Engineering Sciences Data Unit (ESDU) series were utilized. Also utilized were numerical simulation tools including various CFD and FEA software*.

Design Structure Matrix, a modern method of development management, was utilized in order to streamline the design process, form design groups, and monitor the development progress. This method, as described by Eppinger et al. [3], is used to organize interrelated tasks in the design process in a way that minimizes feedback cycles and determines possible parallel analyses. Methods of linear task management were utilized to allow for the parallel configuration development of a family of design concepts.

III. Conceptual Studies

After a broad review of the existing literature pertaining to modern configuration design, two major configuration concepts were identified to have enough performance benefit to justify their implementation and corresponding development risk. It was concluded that the integration of modern propulsion concepts presently being developed, i.e. open fans and geared turbofan engines, could provide substantial performance and operating cost benefits. Natural and hybrid laminar flow technologies were also identified as suitable candidates for implementation as they could significantly improve aerodynamic performance of the configurations. These concepts can greatly reduce an aircraft's fuel burn and emissions; drastically reducing the cost of operation. A family of configurations was developed utilizing these concepts and is shown in Fig. 1.

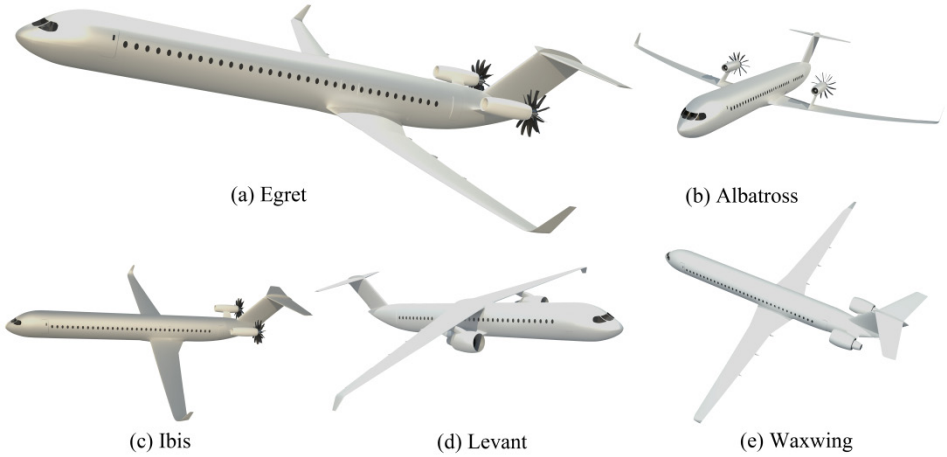

Figure 1. The family of configuration developed by UACC. Egret is the subject of this paper.

* As described in the following sections, numerical procedures were developed to enable analysis of novel concepts in the areas of aeroacoustics and weight engineering.

Egret, Albatross, and Waxwing feature high aspect ratio/low sweep folding wings designed to maximize the extent of NLF on the upper surface of the wing while remaining gate C compatible. Ibis and Levant feature sweep-forward, high aspect ratio wing planforms which help to maintain cleaner outboard boundary layers; reducing drag. Open fan pusher engines are utilized on Egret, Ibis, and Albatross. Albatross features over-the-wing mounted engines. Levant and Waxwing feature geared turbofan engines. While all concepts were developed to a high level of maturity[*], this paper exclusively presents the design process of Egret; featuring the traditional aft-mounted open fan and T-tail empennage. This configuration possesses a moderate development risk, due to the separation of the turbomechanical components from payload, passengers, and critical subsystems, while still utilizing modern technology that will yield substantial reductions in operating costs.

IV. Performance Sizing

To initiate the sizing process, a basic survey of literature was performed to validate NLF as a viable technology to substantiate improvements in L/D within the 2020 timeframe. In particular, papers published by Redeker et al. [4] and Lehner et al. [5] expressed favorable opinions on the availability of NLF technology in this timeframe. Performing a case study analysis, the details of which can be found in the aerodynamics section, it was observed that an 8% reduction in drag at cruise (due only to NLF on the aircraft's wings) would serve as a reasonable estimate for the preliminary mission analysis of Egret [6].

Using the methodology presented by ESDU Performance Data Items 73018 [7], 73019 [8], and 74018 [9], combined with Roskam's [10] low order statistical weight estimation methods, a 13 segment mission analysis was performed using a typical mission profile provided by AIAA [11]. It was assumed that the target improvement in L/D specified by the RFP (25%) was obtained and the Boeing 737-800 was selected as a comparable baseline airplane for the purpose of this mission study. Considering the use of open fan engines, the specific fuel consumption of the engines was reduced by 35%, as claimed by Godston & Reyolds [12][†]. A 3500 nm cruise segment at 36,000 ft and 0.8 Mach was assumed, yielding preliminary Maximum Takeoff Weight (MTOW) of 149,000 lbs and an Operating Empty Weight (OEW) of 75,000 lbs. Using the 2nd order regression methods presented by Roskam [13, 14], as well as the results obtained from the preliminary weight and mission analyses of Egret, initial empirical drag polars were obtained in order to complete preliminary performance sizing. A sizing chart was constructed using the methods presented by Roskam [15], assuming an approach speed of 140 KCAS, a landing distance of 3,500 ft, a takeoff distance of 8,200 ft at a C_L of 2.2, and a maximum cruise speed of Mach 0.83 (340 KCAS). Special attention was given to satisfying all climb requirements stated by Federal Aviation Regulations (FAR) §25.105, §25.111, and §25.121. Figure 2 presents the resulting constraint chart used in the performance sizing of Egret.

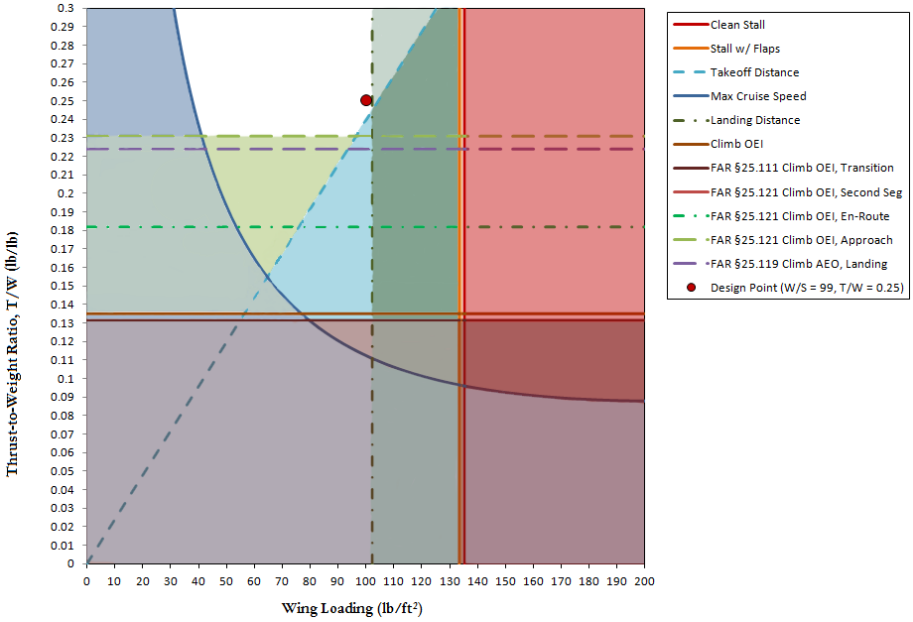

Figure 2. Preliminary Aircraft Sizing. Design space is indicated by the white area.

[*] All concepts were fully developed and entered into the AIAA Team Aircraft Design Competition

[†] These assumptions were refined after detailed aerodynamic and propulsion analysis were performed. It was proven that these assumptions were slightly optimistic.

A thrust to weight ratio of 0.25 and a wing loading of 99 lbs/ft^2 were selected to maximize wing loading, therefore minimizing wing area, while satisfying takeoff distance requirements and all climb gradient requirements as stated by the aforementioned FAR regulations*.

V. Aerodynamics

A. Detailed Analysis of Laminar Flow

Given the substantial increase in weight and complexity cited for hybrid laminar flow devices by Edi et al. [16], as well as the favorable opinions expressed in regards to the feasibility and benefits of NLF concepts by authors such as Lee et al. [18] and Lehner et al. [5], the decision was made to incorporate modern NLF concepts into the aerodynamic design of Egret. Two general strategies were adopted to maximize the extent of NLF. First and foremost, airfoils were to be designed in such a way as to minimize the extent of adverse pressure gradients on the upper surface of the wing, thus extending laminar flow on the wing surface [16]. This strategy will be discussed in the airfoil selection and optimization section. Secondly, it was concluded that by implementing a wing planform with very small leading edge sweep, the effects of cross flow instability† which contributes greatly to the transition to turbulence [16], could be minimized. It is realized that by reducing the sweep of the wing, one might expect an increase in the compressibility component of the aircraft's drag. Considering the fact that the total drag of a commercial aircraft is dominated by friction components at transonic speeds [17], it is argued that a tradeoff exists between increasing the sweep of the wing to reduce compressibility drag and decreasing the sweep to increase NLF at the expense of slightly greater compressibility drag.

The general consensus in literature is that predicting the location of transition to turbulence is an incredibly sophisticated task requiring complex numerical tools or extensive transonic experimentation, which is beyond the capabilities of the UACC. In order to investigate this tradeoff, the empirical method presented by Lehner [19] to estimate the transition location for a transonic wing was used. Equation 1 presents the Lehner's equation that predicts the Reynolds number corresponding to the chordwise transition to turbulence as a function of leading edge sweep.

$$Re_{tr} = 24 \cdot 10^6 - \tan^{-1}\left(\frac{\Lambda_{LE} - 13}{13} \cdot 1.6\right) \cdot \frac{28 \cdot 10^6}{2 \cdot \tan^{-1}(1.6)} \quad (1)$$

B. Airfoil Selection and Optimization

The method for selection of airfoil profiles was dictated by two main elements. First, in order to maximize the extent of NLF on the upper surface, a favorable "rooftop" shape pressure coefficient distribution was sought [4]. Second, the airfoil geometry must be of sufficient thickness to house the wing structure. The upper limits for thickness-to-chord ratio were set to 15% for root, 11% for mid-planform, and 10% for the outboard wing airfoil. In order to obtain a reasonable baseline airfoil, a study of 30 transonic airfoil geometries, available on the University of Illinois Urbana- Champaign's web portal, was conducted. The airfoils were analyzed using the DesignFoil software on the merit of the maximum extent of laminar flow at C_L 0.58 (selected during initial performance sizing). From the initial 30 airfoils studied, eight airfoils were selected for the design. Using the eight final airfoils, 40 combinations of upper and lower surface curves were analyzed in order to select the best performing airfoils. NASA Langley's NLF-415 was selected as the root airfoil profile, the BAC NLF airfoil as the upper profile, and the lower profile of RAE 2822 and SC2110 airfoils were selected as the quarter span and tip airfoils, respectively.

C. Wing Planform Optimization

Based on the NLF method presented, parametric studies were performed in order to obtain the optimal aspect ratio and quarter chord sweep angles that would maximize the L/D of the aircraft, assuming level flight at cruise condition with a lift coefficient of 0.58. A procedure was developed to compute the percentage of laminar flow on the wing as a function of wing area, aspect ratio, and quarter chord sweep angle using Lehner's equation, Eq. (1).

* UACC acknowledges that a more thorough investigation of the design space identified by this constraint chart may yield a more optimal design point if one considers the effect of T/W and W/S on parameters such as Specific Air Range (SAR), Direct operating cost (DOC), and Cash Airplane-Related Operating Costs (CAROC).

† Cross flow instability refers to transition to turbulence caused by the component of the surface flow that travels in the spanwise direction and trips the adjacent flows into increased turbulence levels; therefore increasing the friction drag of the surface.

A parametric analysis was performed by varying the aspect ratio of the wing from 9 to 15 and the quarter chord sweep angle of the wing from 0º to 25º. Considering the results of the airfoil analysis, which indicate that an average 50% laminar flow is achievable* (between upper and lower surfaces of root and tip wing profiles), this analysis was normalized to 50%. Figure 3, presents the results of this parametric study.

In order to perform this analysis, a dynamic configuration file was generated in Advanced Aircraft Analysis (AAA) software. Using the result for the relationship between the extent of the laminar flow and the basic geometry of the aircraft, as well as the inherent geometric and performance sizing capabilities of AAA, a parametric analysis was performed in order to observe the effects of the changes in sweepback angle on the cruise L/D of the configuration. This parametric study was constrained similarly to the laminar flow analysis presented in Fig. 4 so as to preserve consistency. Figure 4 indicates that for any given aspect ratio, there exists an optimal sweep angle that will maximize the cruise L/D. As it can be seen, no particular improvement in cruise L/D is observed as a result of increasing the aspect ratio from 14 to 15; therefore, the aspect ratio was selected to be ~14. The optimal quarter chord sweep angle, accounting for NLF effects, was observed to be ~7-8°. Each data point in Fig. 4 is a fully sized aircraft.

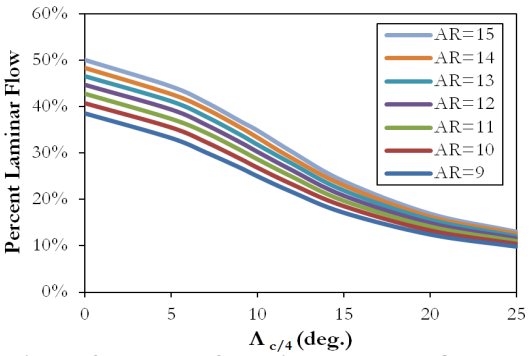

Figure 3. Extent of Laminar Flow vs. Quarter Chord Sweep of the wing.

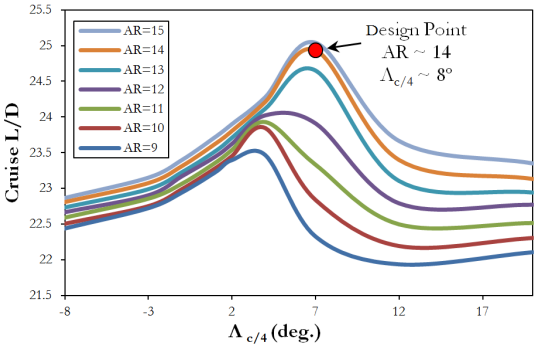

Figure 4. Parametric study of cruise L/D vs. quarter chord sweep of the wing at various aspect ratios. Design point optimal at AR = 14.1 and $\Lambda_{c/4}$ = 8.1°.

D. Numerical Verification of Laminar Flow

To ensure that the wing is capable of sustaining laminar flow on its upper and lower surface, two main elements are required. First, a favorable pressure gradient has to be maintained over a significant portion of the wing planform in the chordwise direction. Second, no shock should exist in the region that laminar flow is expected to be maintained. To verify the capability of Egret's wing planform to satisfy these conditions, a transient Computation Fluid Dynamics (CFD) analysis of the flow field around the wing was performed using COSMOS FloWorks for which the results are presented in Fig. 5. From this analysis, it was concluded that a favorable pressure gradient (i.e. decreasing pressure in the streamwise direction of the flow) exists on the wing upper surface. From the results, it is evident that at cruise the shock on the upper surface does not occur until the 80% chordwise station. The lower surface of the wing is shock free; however, the extent of favorable pressure gradient is smaller than the upper surface.

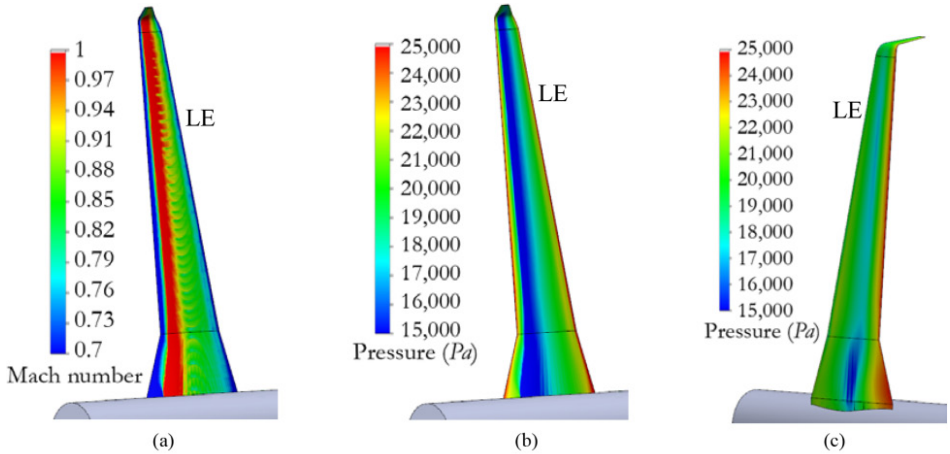

Figure 5. (a) Mach number contours adjacent to the upper surface of the wing. (b) Pressure contours adjacent to the upper surface of the wing. (c) Pressure contours adjacent to the lower surface of the wing.

* This result also agrees with the suggestions made by Lehner et al. [5] regarding normalization of the percentage laminar flow on wing surfaces.

E. High-Lift Device Sizing

The strategy to maintain maximum laminar flow on the wing surfaces dictated that no deployable part on the leading edge should be incorporated. Any sources of flow disturbance, i.e. gaps and misalignments inherent to moving parts, can trip the laminar boundary layer into turbulence. This dictates that only trailing edge high-lift devices can be incorporated; requiring the use of very aggressive multi-slotted flaps with large Fowler motions. Using the Torenbeek [20] method for sizing flaps, a parametric study was performed to determine the required flap chord to wing chord ratio that will generate sufficient C_{Lmax} at takeoff. Figure 6 shows the results of this analysis for flaps having a streamwise extent between 15% and 35% of the wing chord. This parametric study indicated that a flap chord to wing chord ratio of 0.3 is the optimal configuration for a double-slotted Fowler flap, and is capable of generating a C_L of 2.2 at a typical takeoff flap setting and a C_L of 2.3 at a typical approach flap setting.

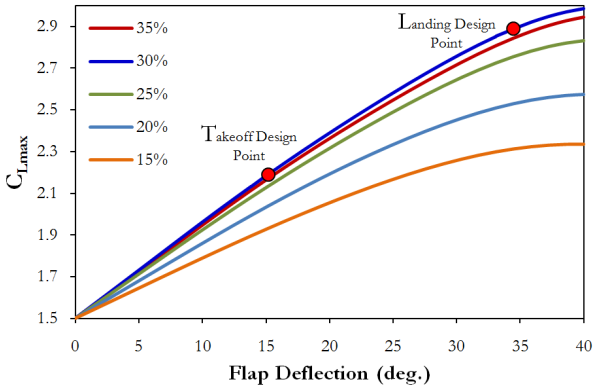

Figure 6. Aircraft maximum lift coefficient vs. flap deflection for different flap chord to wing chord ratios.

F. Detailed Drag Polars and Drag Breakdown

To obtain a more accurate estimate of the lift and drag forces acting on the aircraft, a more detailed analysis of the aircraft's aerodynamics was performed using the methods presented by Roskam [21]. The methodology used to determine cruise drag polars accounts for compressibility effects by taking advantage of the corrections presented in ESDU Transonic Aerodynamic Data Items 6407, 71019, 79004, and 83017 [22-25]. The low speed drag polar methodology was adopted from Torenbeek [26]. The results of the CFD analysis related to the verification of the extent of laminar flow on the wing and fuselage were used to perform a total airplane drag assessment. It was assumed that all empennage surfaces would have 15% of their wetted area exposed to laminar flow. This set of methods was used to estimate the transonic drag for DC-10-40 and verify the accuracy of the results by comparing them to experimental values [27]. It was observed that the utilized methods are capable of predicting the correct drag coefficients with a five percent deviation from experimental values at typical cruise lift coefficient and Mach numbers. Figure 7 presents the results of detailed drag analysis using 5th order drag polar equations, which were also used to verify the satisfaction of performance requirements. This data includes drag coefficients corresponding to a cruise C_L varying from 0.1 to 0.75. The landing C_L represents the C_L required to achieve an approach speed of 140 kts at Maximum Landing Weight (MLW). Figure 8 presents the drag breakdown of Egret at cruise conditions. From the drag breakdown at cruise, it is observed that the drag of the wing constitutes 32% of the drag for the entire aircraft. This number is substantially lower than the conventional 50% wing related drag (including induced drag) at cruise, due to the utilization of NLF.

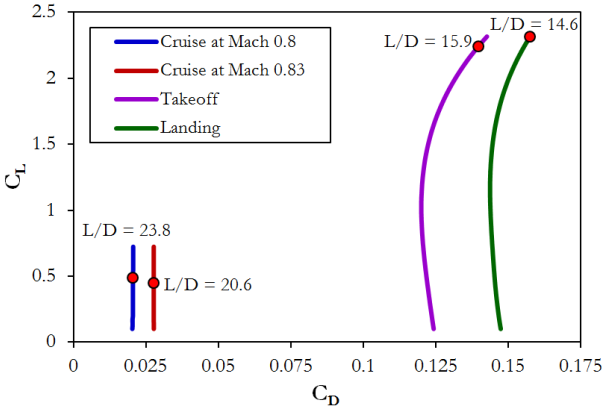

Figure 7. 5th order Drag Polars at Cruise, Max Cruise, Takeoff, and Landing Conditions.

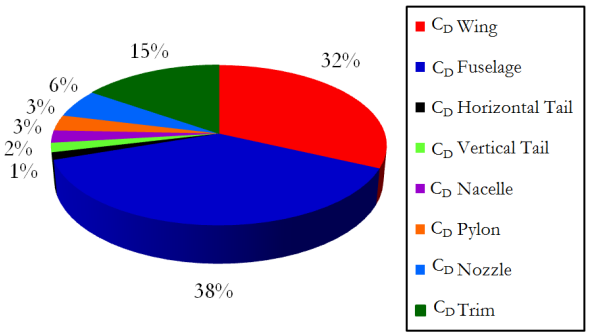

Figure 8. Drag breakdown at cruise.

G. Drag Rise Assessment

Given the low wing sweep resulting from planform optimization, it was critical to verify that the M_{DD} of the configuration exceeds or is equal to the max speed required by the RFP (0.83). Drag rise analysis was performed using the method presented by Roskam [21]. The M_{DD} was defined as the Mach number at which the rate of change of total drag of the aircraft with respect to Mach number exceeds 0.1. Figure 9 presents the results of this analysis.

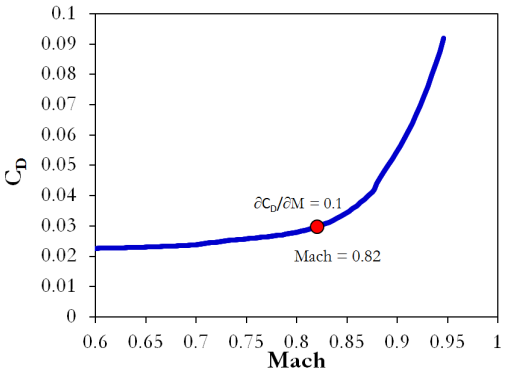

Figure 9. Result of drag divergence analysis on Egret indicating a M_{DD} of 0.82.

VI. Propulsion

Open fan engine concepts, which are considered novel at present, have been under development since the early 80's and may be service ready by 2020 if sufficient demand exists. Furthermore, there exists a business case for the implementation of such engines due to their tremendous potential to reduce specific fuel consumption [28]. Although open fan concepts promise significant reductions in fuel burn and emission levels, they present a new set of issues that need to be addressed if such propulsion concepts are to be used in the near future. According to Holste & Neise [29], the novel arrangement of these engines introduces new sources of acoustic disturbance which contribute greatly towards an increase in noise levels. The potential to have low noise open fan engines has been greatly increased by advancements in aero acoustics, acoustic blade treatment [30], and reduction of rotor induced broadband noise. From the standpoint of configuration, the size and weight of these engines are believed to cause integration issues in the configuration design.

Installation of open fan engines on the rear fuselage concentrates a large portion of the aircraft's empty weight at the rear end; moving the empty aircraft's Center of Gravity (CG) significantly aftward. As a result, the CG of aircraft's freight and payload, i.e. passengers, is located ahead of the empty aircraft's CG. This issue, if not addressed properly, can cause balance problems for aircraft flying with little or no payload. The issues arising from aft-mounted installations were compared against the known wing-mounted configuration concerns such as high cabin noise levels and high speed aerodynamic interferences between the nacelle, rotor, and wings, in order to support an aft mounted configuration.

A. Engine Design

A three spool core configuration was analyzed using the semi-empirical tool GasTurb. Limiting the turbine inlet temperature to 1,440 K, and assuming a burner efficiency of 0.9995 [31] and spool mechanical efficiencies of 0.997, 1, and 0.995 for the high, intermediate, and low pressure spools respectively [32], an 8 compressor stage / 5 turbine stage core configuration was designed as shown in Fig. 10.

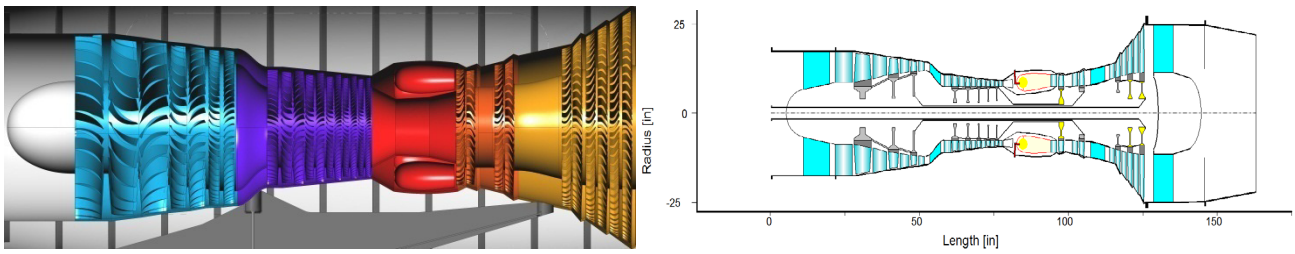

Figure 10. Computer Aided Design (CAD) model cross section (Left) and GasTurb Core Configuration (Right).

A large rotor diameter was selected to obtain a high Bypass Ratio (BPR) for the engine. Analysis shows that this large rotor provides the majority of the engine's thrust, while only a small contribution is produced by the core stream, as will be discussed in the noise section. UACC decided that a contra rotating system would maximize the

rotor propulsive efficiency by minimizing net flow circulation. The two main methods to achieve such a system are a direct drive turbine stage and an epicyclical gearbox. The simpler method utilizes two contra rotating turbines to directly drive each rotor stage. While this system operates optimally at cruise RPM, such a system is not as efficient at other flight conditions such as takeoff because of differing exhaust flow velocity. However, an epicyclical gearbox utilizes a series of gears to generate contra rotating torque and therefore its efficiency is constant and does not depend on the exhaust flow of the turbine. Considering this tradeoff, an epicyclical gearbox system was chosen to create the required contra rotating motion, extracting power from a traditional low pressure turbine shaft as shown in Fig. 11. Analysis using GasTurb indicates that the turbine exhaust temperature will be approximately 700 K (800 ºF), which is sufficiently cooled to substantiate the design of a heated structure for a blade root mechanism using high strength, heat resistive steel alloys [33].

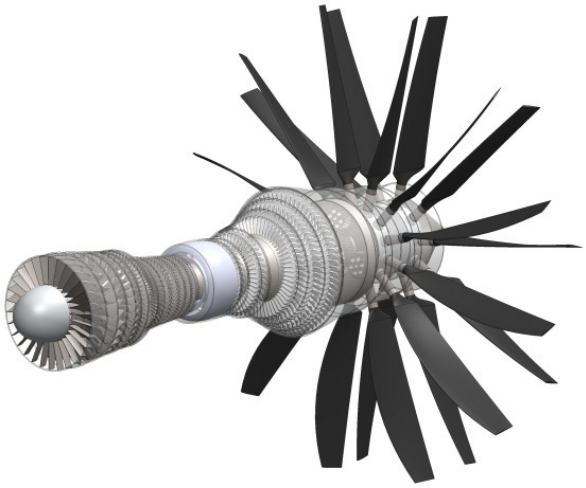

Figure 11. CAD model of the open fan engine.

B. Bleedless Architecture

As stated by Collie et al. [34], the fuel burn of high BPR, small core engines can be significantly reduced by eliminating their bleed air system. Analysis using GasTurb was used to model the effects of the variations of the overboard bleed mass flow on the TSFC of the engine, the results of which can be seen in Fig. 12. By reducing the overboard bleed mass flow from five to zero lbs/sec, the TSFC varies significantly from 0.485 to 0.454 lbs/(lbs-hr) (causing a 6% reduction). Because of this substantial reduction in TSFC, a bleedless architecture was integrated into Egret.

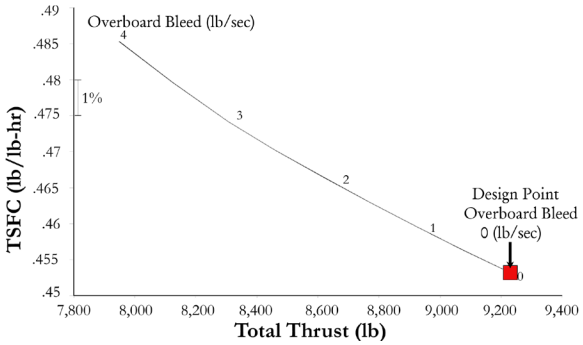

Figure 12. TSFC vs. total thrust at mass flow overboard bleeds from four to zero lbs/sec. The design point suggests minimal TSFC at no overboard bleed.

C. Engine Analysis

Using a sample propeller map presented by Grieb et al. [35], a generic, eight blade, high efficiency propeller map was scaled to obtain a power coefficient of 1.0 and an advance ratio of 1.8 at a propeller efficiency of 0.9 at cruise. A Monte Carlo analysis was performed to identify the optimum combination of burner exit temperature, burner pressure ratio, compressor interdict pressure ratio, altitude, Mach number, and propeller diameter. Using the limits of a Mach number of 0.8 and cruise altitude of 39,000', in addition to the computed drag polars, the engine geometry was optimized to provide the required thrust at those conditions. The engine performance evaluation was repeated to obtain a full engine map characterizing TSFC and available thrust, assuming a 250 kW mechanical power offtake and no bleed air extraction. Intake losses were also modeled using GasTurb. Figure 13 presents this engine map. As seen in Fig.13, in order to maintain sufficient thrust at cruise, the takeoff thrust of the engine is significantly higher than comparably-sized aircraft, such as the Boeing 737 [36]. Therefore, in order to decrease fuel burn and reduce noise, the engines installed on the aircraft may undergo automated derating* depending on operational altitude and speed.

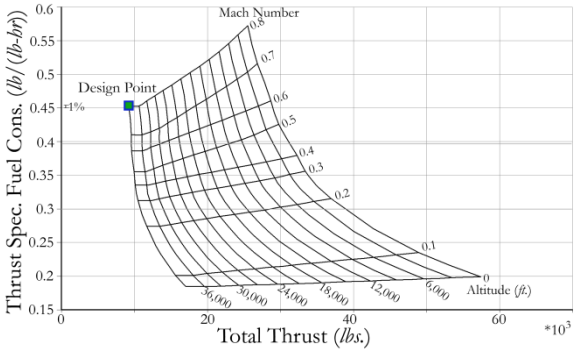

Figure 13. Engine map used for engine performance analysis. Net thrust of the plane is multiplied by two to account for the two engines on Egret.

* Derating refers to the reduction of the maximum available installed thrust of the engine by electronically imposing limitations on the fuel flow of the engine.

D. Engine Integration

In order to effectively integrate the engine, a weight analysis was performed based on a parametric CAD model created for the engine. From this model, the weight of the engine determined by GasTurb was found to be 7,400 lbs, of which 5,500 lbs belong to the engine core and 1,900 lbs belong to the power transmission and rotor system. A mass distribution analysis also indicated that the CG of the core-rotor system is located 49% behind the reference point of the engine, which is fairly aft of the well-established 40% convention for turbo fan engines [37]. The open fan engine concept developed for Egret (mimicking Rolls Royce RB-3011) is considerably heavier than turbo fan engines of the same thrust class. This increase in weight presents difficulties in terms of the structural design of the pylons, as well as the adjacent structure in which the pylons are to be attached. A double spar stabilized pylon was designed in order to install the engine on the aft fuselage.

Using ESDU Data Item 79020 [38], it was determined that a 34" blade clearance from the fuselage would be sufficient to offset the fuselage boundary layer in order to avoid the interference of low energy boundary layer with the fan tips therefore reducing rotor noise and increasing rotor efficiency.

E. Blade Loss Considerations

As required by FAR §25.903, the engine installation has to be done in a manner so that no flight critical items are adjacent to the plane of the propeller or high pressure turbine. This regulation recommends 5º of clearance for rotor blades and 15º for high pressure turbines. Using an analytical model for blade loss, differential equations were developed to model the motion of a blade released from the engine rotor. The analysis goal was to estimate the maximum required clearance angle to investigate the applicability of FAR §25.903 to Egret. Using the model for drag force acting on the blades, UACC has extracted the following differential equation for the velocity of the blade,

$$m_b \dot{v} + P v^2 = 0 \tag{2}$$

where,

$$P = 0.5 C_{D_{blade}} A \varrho, \tag{3}$$

which has solution,

$$v = \left(\frac{1}{v_0} + \frac{Pt}{m_b}\right)^{-1}. \tag{4}$$

Solving for blade motion in two dimensions yields the following equation that models the impingement angle behind the plane of rotation of the rotor,

$$\Omega = \tan^{-1}\left(\frac{m_b}{P_2 D_p} ln\left(\frac{P_2 v_{0,plane}}{P_1 v_{0,prop}}\left(e^{\frac{P_1 D_p}{m_b}} - 1\right) + 1\right) - \frac{m_b v_{0,plane}}{P_1 D_p v_{0,prop}}\left(e^{\frac{P_1 D_p}{m_b}} - 1\right)\right) \tag{5}$$

Inserting relevant values for takeoff, this model indicates that the maximum clearance angle necessary is slightly greater than 1º aft of the plane of blade rotation. This analysis assumes that it is extremely unrealistic for the blade to change its orientation enough to acquire an average radial drag coefficient greater than 0.3 during the fraction of a second it has to make it to the fuselage. This assumption was verified by performing a high speed transient CFD on the blade geometry to investigate the bounds of aerodynamic coefficients (namely C_L and C_D) for the blade. A similar analysis to the takeoff scenario was performed after inserting appropriate values for cruise conditions. The maximum realistic impingement angle was found to be approximately 4.5º aft of the plane of rotation of the blades. Additionally, the analysis shows that there are no likely conditions under which the blade would impact forward of the plane of rotation.

VII. Environmental Considerations

A. Noise

Historically, the noise associated with open fan engines has been a determining factor in preventing them from becoming a mainstream type of commercial aircraft propulsion system. For example, there have been instances where the acoustic pressure from an open fan has worn the paint off nearby points on the aircraft body. Therefore,

considerable analysis has been performed in order to justify the use of open fan engines as well as to provide solutions that will make their use feasible. UACC aims to reduce the noise by 10 Effective Perceived Noise Decibels (EPNdB) compared to the ICAO-4 values [39]. In order to ascertain the feasibility of a reduction of this magnitude, it is necessary to develop an accurate model for the prop fan noise, the most significant contributor to overall noise levels.

Using a method, accurate within 3 dB, presented by Hanson [40], UACC developed an analytic procedure utilizing MAPLE, a symbolic computation software. This model takes into account both harmonic load interactions and acoustic interactions between the two blade rows. Altogether, Hanson's method allows calculation of the complex acoustic interaction between the blade rows, providing an accurate estimation of the largest overall contribution to open fan noise – the inter-row interference component. This approach requires obtaining accurate harmonic lift and drag coefficients for individual blades.

There is no accessible literature within the public domain on a general method to calculate the harmonic lift and drag coefficients for a given blade geometry. Therefore, UACC consulted ESDU Data Item 96027 [41] instead, which provides a method for estimating harmonic lift coefficients due to non-axial inflow into the propeller disk.

Treating the takeoff case and plotting the dB level for several "virtual microphones" placed along the runway, it was determined that the loudest noise is generated when the aircraft reaches takeoff speed and is closest to the observer (450 m. per ICAO-Ch.4). Results indicate a preliminary maximum sideline noise of 109 dB, which considerably exceeds the ICAO Chapter 4 requirement of 94 EPNdB if no noise reduction techniques are utilized.

As a solution, UACC proposed that during takeoff, a clutch mechanism shall disengage the forward blade row on each engine. This eliminates most of the interference noise between the two blade rows. Choosing to disengage the forward rather than aft blade row generates a greater noise reduction, since it is the unsteady flow caused by the forward blade row's rotation that produces the bulk of the interference noise. With this setup, the aft blade row's individual noise contribution needs to be modeled while accounting for the now minor disturbances caused by the stationary forward blade row. A propeller noise estimation presented in the NASA Technical Report 32-1462 [42] gives 76 dB for takeoff conditions with disengaged forward blade rows. This is of course significantly lower than the noise during contra-rotation operations. Though this number seems to be an optimistic estimate, their method is accurate to within 3 dB. At this decibel level, propeller noise is no longer the only considerable contributor to overall noise level. Therefore, other noise sources must be considered to yield a reasonable estimation of the aircraft's total noise level.

Traditional sources of noise include airframe noise, compressor noise, combustor noise, and jet noise. ESDU data items belonging to the noise series [43,44] provide methods to calculate the rest of these sources of noise using empirically verified models. Logarithmically summing these values gives approximately 85 dB for the maximum sideline noise (450 m. offset from the runway). Figure 14 presents the maximum sideline noise breakdown for Egret during takeoff.

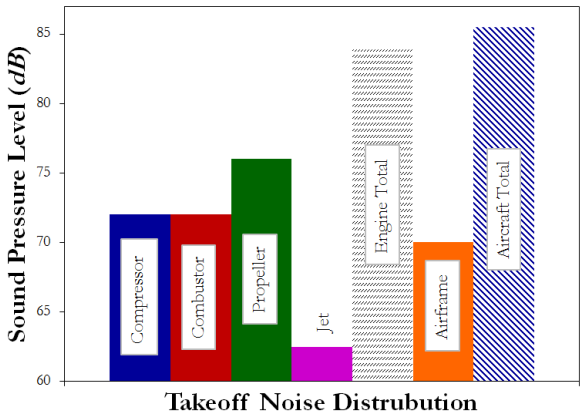

Figure 14. Maximum sideline noise breakdown for Egret during takeoff.

B. Emissions

Considering the possible introduction of carbon taxation in the near future, special attention was given to controlling the emission levels in the design of Egret. It has been suggested that such taxation would be implemented as a part of the tax imposed on the sale of aviation fuel, increasing the cost of fuel for operators of high-emission aircraft. The future market will thus be financially motivated to procure lower emission aircraft.

UACC has addressed the market demands concerning low emission aircraft by using more advanced propulsion technology, flight path optimization, alternative fuels, and general fuel burn enhancements. The modern propulsion concept of open fan engines was selected due to its significant potential to reduce Thrust Specific Fuel Consumption

(TSFC), thus reducing the fuel burn and general emission levels of the aircraft. The NOx intensity factor was chosen as a measure of merit for the production of NOx emissions*, as defined by the Committee of Aeronautical Technologies [45], and is presented in Eq. 6,

$$S_{NO_x} = \left(\frac{P_3}{2965}\right)^{0.4} e^{\left(\frac{T_3-826}{194}+\frac{6.29-100war}{53.2}\right)} \quad (6)$$

An analysis was performed using GasTurb to evaluate the NOx severity factor over the flight envelope of the engine of the aircraft, the result of which is shown in Fig. 15. From this analysis, it was determined that 5.75 grams of NOx is generated per every kilogram of fuel burned at 39,000' altitude. Emphasis was placed on optimizing the flight path of the aircraft [46] in order to reduce the fuel burn and corresponding emission levels by accurately determining the optimum cruise Mach number and altitude (within the range specified by the RFP). Utilizing modern structure and NLF technology contributed to reductions in weight and an increase in the L/D of Egret, consequently providing a significant reduction in the fuel burn and emissions of the aircraft.

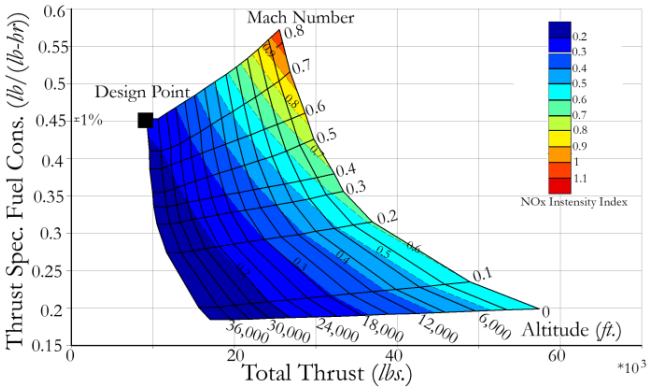

Figure 15. NOx intensity contours plotted over engine performance map.

C. Biofuels

The implementation of an environmental tax, which has reasonable likelihood of occurring by 2020, requires a solution to reduce the influence of such a tax on the cost of commercial flight. Methods of reducing emissions include increasing the efficiencies of the propulsion system and utilizing NLF technologies, both of which are present in Egret. This already significant reduction can be augmented by the use of low carbon footprint fuels, i.e. biofuels. The use of such fuels can result in an 80% reduction in the net carbon output, and a corresponding reduction in carbon taxation [47].

For their benefits, biofuels also present some challenges. If their biological sources are not chosen carefully, they could compete with food crops for arable land, which is not a sustainable option. Additionally, an ideal biofuel would require no modifications to aircraft or infrastructure of the airports [48]. As a result of these requirements, the ideal biofuel would consist of Hydrotreated Renewable Jet (HRJ) derived from sources such as japtropha, camelina, algae, and halophytes [49]. It is created by extracting and filtering the oil from the feedstock and then heating and hydro-treating it to correct its molecular structure [50].

VIII. Material Selection

After considering the three main factors of weight, manufacturing methods, and near field acoustic fatigue tolerance, UACC determined that the optimum structural material for the Egret should be composites. The weight reduction due to aggressive utilization of advanced materials will improve the general fuel economy performance by reducing the induced drag of the aircraft due to less required lift to maintain steady flight.

Given the high level of near-field acoustic disturbances associated with open-fan engines [29], acoustic fatigue of structures adjacent to the rotor-blades is critical in the design of the airframe. The ESDU Data Item 84027 [51] demonstrated that aluminum laminate-based composites, such as GLARE, have a very high tolerance when exposed to continuous, random acoustic loading. The material distribution is shown in Fig. 16.

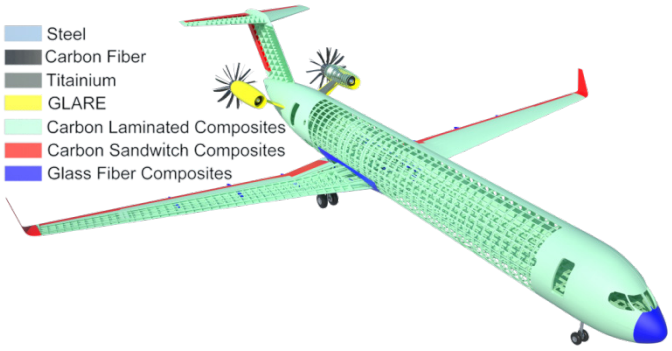

Figure 16. Material distribution diagram.

* NO_x was chosen because it is particularly damaging to the ozone layer when produced at cruise altitudes [46].

IX. Weight & Balance

A. Folding Mechanism

As requested by the RFP and in order to maintain compatibility with worldwide conventional airport infrastructure, Egret was equipped with a folding wing mechanism, as shown in Fig. 17. The outboard 19.5' of the wing can be folded while on the tarmac to reduce the overall wingspan to 118'. The weight increase figures were normalized from the Boeing 777's empty weight and applied to the weight estimations of Egret, resulting in an 800 lbs increase in the wing structure.

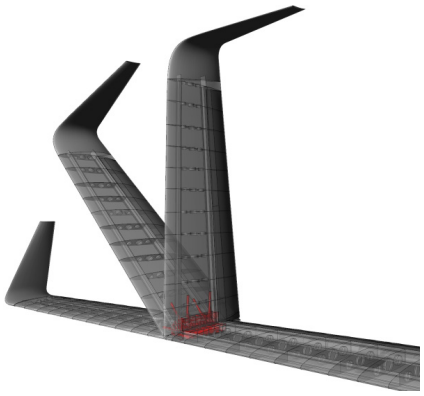

Figure 17. Folding mechanism operation.

B. Fuselage Acoustic Insulation Weight Increment

In light of data obtained from the NASA Propfan Test Assessment project overview [52], excessive interior noise levels can be expected due to the proximity of the open rotor blades to the cabin. To remedy this, additional noise insulating material will be required inside the cabin wall lining to absorb the excessive acoustic energy. The method presented by Wilby et al. [53] was used to approximate the weight penalty from additional noise insulation in the mid fuselage section. This weight increment was added to the averaged weight figures for the fuselage structure.

C. Final Weight Analysis

The initial estimates were averaged with the General Dynamic and Torenbeek methods [54] then fed into an iterative algorithm. The impact of lightweight composites was estimated by comparing the reduced weight of Boeing 787 components against the components of similar-sized aircraft. The differences were applied to Egret's weight estimation. The additional weight penalties due to unique aircraft components, such as the folding wingtips and open fan noise insulation, were normalized with the weight reductions that resulted from an all-electric architecture [55], verified by the relevant literature, and then applied to Egret. The results are shown in Table 1.

Table 1. Takeoff weight summary.

W_{fix}	$W_{Structure}$	W_{PP}	$W_{F,max}$	OEW	MTOW
24,160 lbs	34,530 lbs	16,190 lbs	37,340 lbs	76,880 lbs	151,220 lbs

D. CG Travel

Static stability of the configuration was achieved by performing a parametric study of the impact of the longitudinal location of the wing on the magnitude of static margin using the methods presented by Roskam [56]. Mass properties analysis of Egret indicated that a CG travel range equivalent to 22% of mean aerodynamic chord of the aircraft is likely in a maximum range mission. A target rigid body stick free static margin of 18%* was selected for the mid-cruise segment of the flight to ensure the inherent static stability of the aircraft considering the location variations of the CG during flight. The result of this parametric study can be seen in Figure 18. UACC concluded that a longitudinal wing

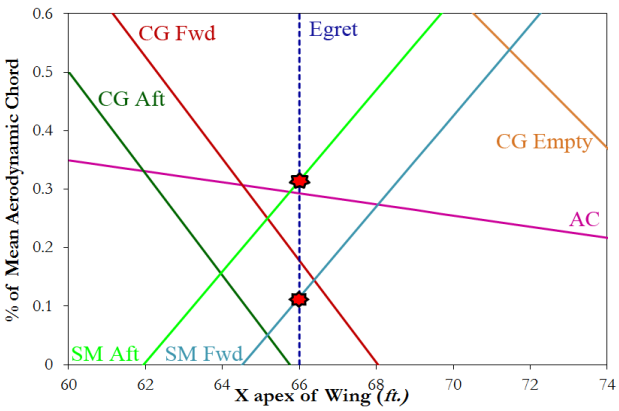

Figure 18. Wing location trade study.

* Per suggestion of Mr. Mark Page, Chief Scientist, Swift Engineering.

apex of 66' will provide sufficient positive static margin at forward and aft locations of the CG, therefore ensuring the maintenance of the static stability of the aircraft under all loading conditions.

X. Performance

A. Field Performance

The required takeoff field length for Egret was determined by applying relations presented by ESDU Data Item 85029 [57] and considering the ground effect on generated lift and drag [58]. It is assumed that the aircraft uses only the trailing edge flaps during takeoff without assistance from leading edge high lift devices, making the maximum lift coefficient (C_{Lmax}=2.2) attainable. The average kinetic friction coefficient during ground roll was computed using the data presented by Roskam [59] to be 0.02, assuming a conventional tarmac mix used in the United States. Using these methods, the overall takeoff field length was computed to be 7,300 feet, the ground roll 5,000 feet, and a liftoff speed 137 kts. Worth mentioning is that Egret exceeds 8,200 feet takeoff field length requirement substantially. The large thrust lapse associated with high bypass ratio propulsion systems dictates that the engines have to be sized for cruise conditions, which leads to excess thrust at takeoff.

B. Fuel Burn Performance

Detailed analysis of the block fuel burn was performed to assess the economic advantages of Egret over present day technology. Analysis was repeated for three different block ranges of 850, 1,200, and 3,500 nmi for 175 passengers, which is equivalent to a payload of 37,000 lbs. Figure 19 presents the results of this analysis. From this figure it is evident that for longer range missions, significant reductions in block fuel burn are attained by flying at higher initial cruise altitudes. The initial cruise altitude has a very minute effect on the block fuel burn of the aircraft for shorter ranges, such as the 1,200 nmi nominal block range specified by the RFP. This analysis also confirmed that the block fuel burn for a 1,200 nmi mission with 175 passengers is approximately 5,900 lbs., assuming an initial cruise altitude of 39,000' and a fuel burn per passenger of 33 lbs/seat. This value is almost 6 % lower than the goal set by NASA N+1 study [60] which confirms that the power plant technology level selected for Egret is capable of satisfying the market's needs

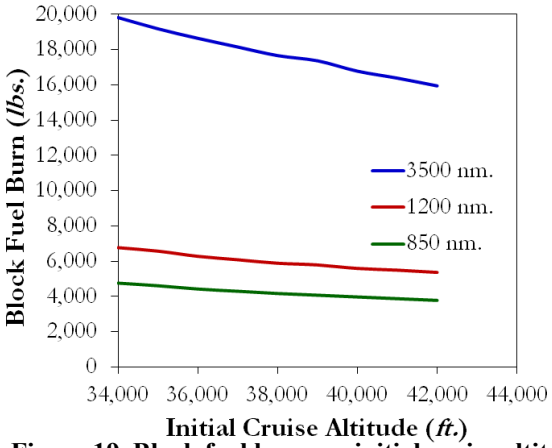

Figure 19. Block fuel burn vs. initial cruise altitude.

XI. Cost Analysis

A. Environmental Tax Modeling

In order to include the effects of the proposed environmental taxation methods on the aircraft's Direct Operating Cost (DOC) and Cash Airplane-Related Operating Costs (CAROC), a method based on the work presented by Schwartz et al. [46] was adopted and used to perform the flight path optimizations presented. This method accounts for four main components of the environmental tax. The most significant component is the carbon tax, which is computed as 0.33¢ per gallon fuel burned. Schwartz suggests that the carbon emissions, for any given propulsion system, are a linear function of fuel burn, and therefore are independent of altitude*. The combined taxation accounting for NOx emissions, Aviation Induced Cloudiness (AIC), and high altitude cirrus

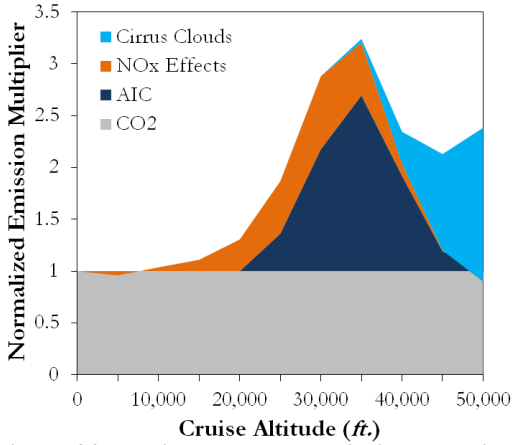

Figure 20. Environmental multiplier vs. altitude.

* Note that the variation of altitude has a significant effect on the block fuel burn in long range flights, therefore affecting the total carbon emissions of the airplane.

clouds were computed as a multiplier to be added to the baseline carbon tax (as a fraction). Given that Schwartz provides values for the variation of the influence of each of these forms of emissions as a function of altitude, her model was adopted to compute the total environmental tax imposed on the operation of the aircraft. Figure 20 presents the variation of taxable pollutants normalized to one, based on CO2 emissions, which are assumed constant, independent of altitude. Equation 7 is used to compute the environmental tax in U.S. dollars,

$$C_{ENVTAX} = 0.33 \cdot (1 + \sum_{i=1}^{3} M_i) \tag{7}$$

where M_i is the corresponding normalized emission multiplier as shown in Fig. 20.

B. Flight Path Optimization

Multiple parametric studies were performed in order to optimize the mission profile. Given that the aircraft is expected to perform transport missions in a variety of ranges, a parametric study was performed to optimize cruise Mach number and initial altitude for both the 1,200 nmi nominal and 3,500 nmi maximum design ranges. In order to model the direct operating cost of the aircraft as a function of the mission variables, such as average block speed and initial cruise altitude, the financial model provided by Roskam [61] for estimation of the Research Development Testing and evaluations (RDTE), acquisition, and operating costs was programmed into a dynamic spreadsheet. The previously mentioned model for environmental tax was also utilized to take into account the effects of flight path parameters on the DOC of Egret. Considering the previously mentioned results for the engine optimization, the DOC and the corresponding aircraft unit cost were computed for a range of Mach numbers and initial cruise altitudes. The result of these analyses is shown in Fig. 21.

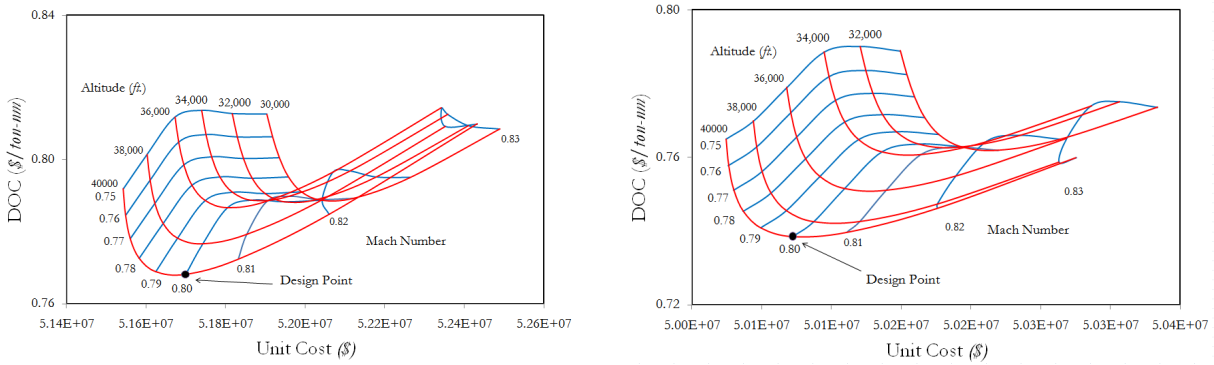

Figure 21. DOC vs. unit cost for various initial cruise altitudes and Mach numbers, at a range of 3,500 nmi (Left). DOC vs. unit cost for various initial cruise altitudes and Mach numbers, at a range of 1,200 nmi (Right). Both for a production run of 500 Aircraft.

The analysis indicates that the DOC for maximum range missions rapidly declines as the aircraft starts to fly at higher altitudes, and is minimized at a Mach number of 0.79 to 0.8. In the 1,200 nmi nominal range case, the DOC does not reduce as rapidly as the aircraft flies at higher altitudes. Instead of a Mach number of 0.79 to 0.8, the DOC would be minimized at a Mach number of 0.8 to 0.81. The analysis also indicates that the unit cost of Egret for a production run of 500 aircraft will be impacted slightly by the chosen flight path parameters. This is due to the impact of the design Mach number and altitude on the structural weight of the aircraft, which in turn impacts the unit cost.

UACC recommends that Egret should be flown at a Mach number of 0.81, while flying missions near the nominal range of 1,200 nmi. The results of the analysis presented in Fig. 21 indicate that the reductions in DOC due to increasing Initial Cruise Altitude (ICA) are minimal above an altitude of 39,000'. Therefore, UACC recommends an ICA of 39,000' for Egret; however, higher cruise altitudes, if allowed by Air Traffic Control (ATC), will still improve the DOC of the aircraft. While flying missions near the maximum range of 3,500 nmi, the aircraft will incur less cost and cause less environmental impact if it is operated at a lower Mach number of approximately 0.79 and the highest altitude allowed by the ATC and aircraft performance (43,000 feet).

C. Operating Cost Breakdown & Competitive Analysis

As requested by the RFP, the operation and maintenance costs of Egret were computed to assess its viability against current in-service aircraft. Roskam's [62] method was used to perform DOC estimation for Egret using both biofuels and conventional JP-10 jet fuel. The cost of regular fuel was obtained by consulting the fuel cost projections obtained from the U.S. Energy Information Administration interactive web portal [63]. This portal presents projections for the cost of energy and main forms of fossil fuels assuming different economic scenarios by modeling

observed trends in energy supply and demand cycles. Reviewing these projections, it was determined that in 2020, an average jet fuel cost of 2.98 $/gal. will represent the middle ground between the worst and best economic scenarios. A study by E4tech Company [64], suggests that biofuels are cost comparable at present, but their demand will greatly exceed the production volume if they become commercially available. This study also indicates that the cost of HRJ related biofuels could be as low as 1.20 $/gal. Moreover, the maximum cost for HRJ related biofuels is considered to be dictated by the cost of jet fuel (which can be as high as 2.98 $/gal) to preserve competitiveness in the energy market. Furthermore, the study suggests that HRJ related biofuels will be available commercially by 2018, implying that by 2020 these biofuels will be substantially cheaper than conventional aviation fuel. UACC concluded from this study that a cost of 2.09 $/gal. for HRJ related biofuels was an accurate projection. The environmental tax model presented earlier was implemented to account for the benefits incurred by utilization of lower carbon footprint biofuels and flying at higher altitudes, which will reduce emission tax.

DOC analyses were performed for Egret using both conventional aviation fuel and HRJ related biofuels. Similar cost estimations were performed on the Boeing 737 and Airbus A320 to compare annual utilization times. Table 2 presents the results of DOC comparison analyses for a production run of 500 aircraft.

Table 2 Results of DOC comparison.

Cost Item	Airbus A320-200	Boeing 737-800	Egret (Jet Fuel)	Egret (Biofuels)	Average Change from Today's Competitors (Jet Fuel, Biofuels)
Annual Utilization (nmi)	1,865,256	1,891,081	1,807,932	1,807,932	-3.7%, -3.7%
Crew ($/nmi)	0.96	0.95	0.91	0.91	-4.8%, -4.8%
Fuel, Oil, & Env. Tax ($/nmi)	4.53	3.85	2.28	1.6	-46%, -62%
Insurance ($/nmi)	0.15	0.15	0.31	0.42	+107%, +180%
Maintenance ($/nmi)	2.96	2.84	2.42	2.42	-17%, -17%
Depreciation ($/nmi)	4.93	4.68	2.77	1.56	-42%, -68%
Landing & Navigation Fees ($)	0.4	0.36	0.22	0.22	-42%, -42%
Total DOC ($/nmi)	15.03	13.85	8.91	7.13	-38%, -51%

From this analysis, it was concluded that Egret will present significant reductions in DOC thanks to improvements in TSFC (~25%) and cruise L/D (~30%) due to the utilization of modern technologies, such as open fan engines and NLF wings. It is also shown that the DOC of Egret could be reduced by as much as 13% as a consequence of using biofuels. It should be noted that this analysis is only valid for the 2020 market, and this difference will increase as oil prices rise and HRJ related biofuels become more available economically.

XII. Conclusion

It is observed that by implementing advanced concepts in a novel aircraft configuration significant improvements in DOC (38%) can be achieved while meeting today's performance standards. The improved DOC is achieved through a reduced TSFC (~25%) and increased cruise L/D (~30%). If environmental taxation is considered, it is projected that a further 13% improvement in DOC (total of 51%) can be reached through the use of biofuels. There are inherent development risks associated with the utilization of substantially new technology. However, these risks can be mitigated through the substantial increase of profit margins for the airlines and an expect growth in the narrow-body medium range aircraft. The full proposal of Egret can be found at http://issuu.com/sina_golshany/docs/egret.

Acknowledgements

Having completed this project, we would like to express our appreciation of the help and support given by the faculty of USC's aerospace and mechanical engineering department. First of all, we wish to thank the people who were integral to the conception of this project: Dr. Ron Blackwelder, Mr. Blaine Rawdon, and Mr. Mark Page. With their experience in the field of aircraft design, they have been very supportive in all the phases of this project. During the first months of his retirement, Dr. Ron Blackwelder contributed greatly to all aspects of this project, including technical and organizational support for team members.

Several people have been instrumental in allowing this project to be completed, but above all, we are indebted to: Professors Larry Redekopp, Oussama Safadi, Fokion Egolfopoulos, and David Wilcox who backed our efforts over the past year. We would also like to thank two individuals within the Boeing Company who provided

encouragement to begin this project: Dr. David J. Paisley, and Mr. Perry Rea. Among many others we would like to thank Dr. David Glasgow at the University of Southern California's office of undergraduate research and the Los Angeles branch of the AIAA chaired by Dean Davis for providing us with the essential funding for this research project to proceed.

References

[1] Roskam, Jan., *Airplane Design*, Part I through VIII , DAR Corporation, 2003
[2] Heinemann, E., Raussa, R. and Van Every, K., *Aircraft Design*, The Nautical and Aviation Publication Co., 1985
[3] Eppinger, Steven D. and Ulrich, Karl T. *Product Design and Development*, Second Edition, Irwin McGraw-Hill, Boston, 2000.
[4] Redeker, G., Horstmann, K.H., Köster, H., and Quast A. Investigations on High Reynolds Number Laminar Flow Airfoils. *Journal of Aircraft* Vol. 25 № 7. July 1988.
[5] Lehner, Stephan and Crossley, William. "Hybrid Optimization for a Combinatorial Aircraft Design Problem," *Proceedings of 9th AIAA Aviation Technology, Integration, and Operations Conference*. 21-23 September 2009.
[6] Roskam, Jan. *Airplane Design Part VI* Sec. 4.2 p. 23-43. DAR Corporation. 1990.
[7] "Engineering Science Data Unit". *Volumes on Performance*, item 73018. "Introduction to Estimation of Range and Endurance".
[8] "Engineering Science Data Unit". *Volumes on Performance*, item 73019. "Approximate Methods for Estimation of Cruise, Range, and Endurance".
[9] "Engineering Science Data Unit". *Volumes on Performance*, items 74018. "Lost Range, Fuel, and Time Due to Climb and Descent".
[10] Roskam, Jan. *Airplane Design, Part V* Ch. 2 p. 3-17. DAR Corporation. 1999.
[11] Appendix to Request for Proposal Document for Team Aircraft Design Competition. AIAA. 2008-2009.
[12] Godston, J., and Reynolds, C. "Propulsion System Integration Configurations for Future Prop-Fan Powered Aircraft," *Proceedings of AIAA/SAE/ASME 19th Joint Propulsion Conference*. Seattle Washington. June 27-29. 1983
[13] Roskam, Jan. *Airplane Design Part I*, Sec. 341 p. 118-187. DAR Corporation. 1997.
[14] Roskam, Jan. *Airplane Design Part II,* Fig. 12.7 p.286. DAR Corporation. 1997.
[15] Roskam, Jan. *Airplane Design Part I*, Sec. 3.2 p 94. DAR Corporation 1997.
[16] Edi, Prasetyo, Fielding, J.P. "Civil-Transport Wing Design Concepts," *Journal of Aircraft*, Vol. 43, № 4. July-August 2006.
[17] Huenecke, Klaus. *Modern Combat Aircraft Design*. p. 47 fig. 4-14. Airlife Publishing Ltd. England. 1987.
[18] Lee, Jae-Moon, Schrage, Daniel and Mavris, Dimitri. "Development of Subsonic Transports with Natural Laminar Flow Wings," *AIAA Journal 98-0406*. 1997.
[19] Lehner, S., and Crossley, W. "Combinatorial Optimization to Include Greener Technologies in a Short-to-Medium Range Commercial Aircraft." *ICAS 2008-4.10.2, ICAS 2008 Congress including the 8th AIAA 2008 ATIO Conference*. Anchorage, AK. September 15-18, 2008.
[20] Torenbeek, E. *Synthesis of Subsonic Airplane Design*. Appendix G, p. 533. 1981
[21] Roskam, Jan. *Airplane Design. Part VI*. DAR Corporation. 1990.
[22] "Engineering Science Data Unit". *Volumes on Transonic Aerodynamics*, items 6407. "A Method of estimating Drag-Rise Mach Number for Two-Dimensional Aerofoil Sections".
[23] "Engineering Science Data Unit". *Volumes on Transonic Aerodynamics*, items 71019. "Drag-Rise Mach Number of Aerofoils having a Specified form of Upper-Surface Pressure Distribution: Charts and Comments on Design".
[24] "Engineering Science Data Unit". *Volumes on Transonic Aerodynamics*, items 79004. "Forebodies of Fineness Ratio 1.0, 1.5 and 2.0, Having Low values of Wave Drag Coefficient at Transonic Speeds".
[25] "Engineering Science Data Unit". *Volumes on Transonic Aerodynamics*, items 83017. "The Wave Drag Coefficient of Spherically Blunted Secant Ogive Forebodies of Fineness Ratio 1.0, 1.5 and 2.0 at Zero Incidence in Transonic Flow".
[26] Torenbeek, E. *Synthesis of Subsonic Airplane Design*. 1981.
[27] Morgan. *Turbojet Fundamentals*. Douglas Aircraft Company, Inc. Santa Monica, CA. 1956.
[28] McKay, Bruce.ds, C. "Next Generation Propulsion & Air Vehicle Considerations," *Proceedings of AIAA/SAE/ASME 19th Joint Propulsion Conference.* Denver Colorado. August 2-5. 2009.
[29] Holste,F. and Neise, W, "Noise Source Identification in a Propfan Modeled by Means of Acoustic Near Field Measurements", *Journal of Sound and Vibration* №203(4), 1997.

[30] Shivashankara B., Johnson, D., and Cuthbertson, R. Installation Effection on Counter-Rotation Propeller Noise. Boeing Commercial Airplanes. *Proceedings of AIAA 13th Aeroacoustic conference*. October 22-24, 1990.
[31] Rangwala, A.S. *Turbo-Machinery Dynamics: Design and Operation*. McGraw Hill. 2005.
[32] Cumpsty, Nicholas. *Jet Propulsion: A simple guide to the aerodynamic and thermodynamic design and performance of jet engines.* Second Edition. Cambridge University Press. Ch. 11. 2003.
[33] Giampaolo, Tony. *Gas Turbine Handbook: Principles and Practice*. Taylor and Francis. 2009.
[34] *Collie*, *WallisV*., et al. Advanced Propulsion System Design and Integration For a Turbojet Powered Unmanned Aerial Vehicle. Proceedings of the 41st Aerospace Science Meeting and Exhibit. Reno, Nevada. January 6-9. 2003.
[35] Eckardt, D. and Grieb, H. *Turbofan and Propfan as Basis for Future Economic Propulsion Concepts*. Proceedings of AIAA/ASME/SAE/ASEE 22_{nd} Joint Propulsion Conference. Huntsville, Alabama. June 16-18. 1986.
[36] Boeing 737 Specification Sheet, BCA Division, http://www.boeing.com/commercial/737family/specs.html.
[37] AAA, Advanced Aircraft Analysis, Software Package, Ver 3.20, DAR Corporation, Wichita, KS, 2010.
[38] "Engineering Science Data Unit". *Volumes on Aerodynamics*, item 83017 Amendment A. "The Influence of Body Geometry and Flow Conditions on Axisymmetric Boundary Layers at Subcritical Mach Numbers." Amendment A. September, 1984.
[39] Annex 16 to the conventions on International Civil Aviation, Volume I, Aircraft noise, P. II.3.3 dated 20/11/2008, International Civil Aviation Organization.
[40] Hanson, D.B. Counter Rotation Propellers. *Proceedings of AIAA/NASA 9th Aeroacoustics Conference.* October 15-17, 1984.
[41] "Engineering Science Data Unit". *Volumes on Aircraft Noise,* item 96027. Estimation of the Unsteady Lift Coefficient of Subsonic Propeller Blades in Non-axial Inflows. May 1997.
[42] Marte, Jack E. and Kurtz, Donald W. *NASA Technical Report* 32-1462. A Review of Aerodynamic Noise from Propellers, Rotors, and Lift Fans. Jet Propulsion Laboratory. January 1970.
[43] "Engineering Science Data Unit". *Volumes on Aircraft Noise*, item 90023. Amendment D. Airframe Noise Prediction. December 2008.
[44] "Engineering Science Data Unit". *Volumes on Aircraft Noise*, item 05001. Prediction of Combustor Noise from Gas Turbine Engines. February 2005.
[45] Committee of Aeronautical Technologies, Aeronautics and Space Engineering Board, *Commission on Engineering and Technical Systems*, National Research Council of Aeronautical Technology for the Twenty-First Century National Academy Press, Washington, D.C. 1992.
[46] Schwartz, Emily and Kroo , Ilan M. Aircraft Design: Trading Cost and Climate Impact. *Proceedings at the 47^{th} AIAA Aerospace Science meeting*, Stanford University Jan. 5-9, 2009.
[47] International Air Transport Association. *International Air Transport Association Report on Alternative Fuels*. p. 1. 2009.
[48] International Air Transport Association. *International Air Transport Association Report on Alternative Fuels*. p. 34. 2009.
[49] Air Traffic Action Group. *Beginner's Guide to Aviation Biofuels*. p.6. May 2009.
[50] E4tech. *Review of the Potential for Biofuels in Aviation for the Committee on Climate Change*. P. 37. August 2009.
[51] "Engineering Science Data Unit". *Volumes on Acoustic Fatigue,* item 84027. "Endurance of Fibre-Reinforced Composite, Laminated Structural Elements Subjected to Simulated Random Acoustic Loading". Amendment C. August, 2001.
[52] Graber, Edwin J. *Overview of NASA PTA Propfan Flight Test Program*. NASA report number N92-22536.
[53] Wilby, J.F., Rennison, D.C., and Wilby, E.G. Noise Control Predictions for High Speed, Propeller-Driven Aircraft. *Proceedings of the 6th AIAA Aeroacoustics Conference.* June 4-6. 1980.
[54] Roskam, Jan. *Airplane Design Part V*. Section 5. 1999
[55] Cronin, Michael J. All-*Electric vs Conventional Aircraft: The Production/Operational Aspects*. Lockheed California Co. June, 1983.
[56] Roskam, Jan. *Airplane Flight Dynamics and Automated Flight Controls*. Part I Sec. 4.2.2. p. 205. 2003.
[57] "Engineering Science Data Unit". *Volumes on Performance*, item 85029. "Calculation of Ground Performance in Takeoff and Landing". Amendment A. March 2006.
[58] "Engineering Science Data Unit". *Volumes on Performance,* item 85029. "Calculation of Ground Performance in Takeoff and Landing". Amendment A. March 2006.
[59] Roskam, Jan. *Airplane Design Part VII* Sec. 5.2 p. 117-123. DAR Corporation. 1991.

[60] Berton, Jeffrey J., and Envia, Edmane. An Analytical Assessment of NASA's N+1 Subsonic Fixed Wing Project Noise Goal. *Proceedings of the 15th AIAA/CEAS Aeroacoustics (30th AIAA Aeroacoustics) Conference*. May 11-13, 2009.
[61] Roskam Jan., *Airplane Design Part VIII* ; Section 5.2.4; DAR Corporation. 1990.
[62] Roskam, Jan. *Airplane Design Part VIII*. DAR Corporation 1990.
[63] U.S. Energy Information Administration, Independent Statistics and Analysis. *Annual Energy Outlook*. May 11, 2010.
[64] E4tech. *Review of the Potential for Biofuels in Aviation for the Committee on Climate Change*. P. 76. August 2009.